Design Concepts and Performance of NASA X-Band (7162 MHz/8415 MHz) Transponder for Deep-Space Spacecraft Applications

N. R. Mysoor, J. D. Perret, and A. W. Kermode
Spacecraft Telecommunications Equipment Section

This article summarizes the design concepts and measured performance characteristics of an X-band (7162-MHz/8415-MHz) breadboard deep-space transponder (DST) for future spacecraft applications, with the first use scheduled for the Comet Rendezvous Asteroid Flyby (CRAF) and Cassini missions in 1995 and 1996, respectively. The DST consists of a double-conversion, superheterodyne, automatic phase-tracking receiver, and an X-band (8415-MHz) exciter to drive redundant downlink power amplifiers. The receiver acquires and coherently phase tracks the modulated or unmodulated X-band (7162-MHz) uplink carrier signal. The exciter phase modulates the X-band (8415-MHz) downlink signal with composite telemetry and ranging signals. The receiver measured tracking threshold, automatic gain control, static phase error, and phase jitter characteristics of the breadboard DST are in good agreement with the expected performance. The measured results show a receiver tracking threshold of −158 dBm and a dynamic signal range of 88 dB.

I. Introduction

Telecommunication transponders for deep-space spacecraft applications provide independent uplink command and turnaround ranging functions, as well as downlink telemetry and radiometric capabilities. The spacecraft deep-space transponder (DST) is an element in the overall Deep Space Network (DSN) system. A balanced design approach for all the elements of the system must be applied to achieve end-to-end system performance capabilities that include telecommunications and radiometric functions and multichannel and multifrequency capabilities [1]. The DST functions include:

(1) precision phase/frequency reference transfer from the uplink signal

(2) demodulation of the command and ranging signals from the uplink carrier

(3) generation of a coherent or noncoherent downlink tracking signal for the Earth-based DSN

(4) providing downlink signal modulation with composite telemetry data and turnaround ranging or differential one-way ranging (DOR) signals

(5) providing a functional capability to utilize an external ultrastable oscillator (USO) to generate the downlink signal

This article describes the design, implementation, and performance of a breadboard DST configuration. The design specifications and functional description of the DST are summarized in Section II. The DST block diagram is described in Section III. The experimental results of a breadboard DST are presented in Section IV. Finally, some conclusions are drawn in Section V.

II. Key Design Requirements

The design requirements for the DST are summarized in Table 1. The DST is to provide a receive and transmit capability at X-band (7162 MHz/8415 MHz) with the necessary reference signals to generate independent S-band (2295-MHz) and Ka-band (31,977-MHz) downlink signals external to the DST. Frequency translation ratios have been selected to provide coherent operation at S-band, X-band, and Ka-band, with overlap in all three frequency bands for simultaneous coherent operation. The selected transmit/receive frequency translation ratio for DST coherent operation at X-band (8415 MHz down, 7162 MHz up) is 880/749. The DST received uplink is at an assigned channel in the frequency range from 7145 to 7190 MHz (749 F_1). The DST X-band (880 F_1 = 8415 MHz) downlink frequency for the corresponding frequency channel assignment is in the frequency range from 8400 to 8450 MHz (Table 1). The receiver performance requirements include a maximum noise figure of 2.5 dB, a tracking threshold level of -158 dBm, and a tracking range of ± 250 kHz at the assigned channel frequency. The acquisition and tracking rate is 550 Hz/sec at signal levels greater than -110 dBm. The specified nominal output power of the exciter is +12.5 dBm. The exciter output is phase modulated to a maximum phase deviation of ± 2.5 rad with a radio frequency (RF) modulation bandwidth greater than 40 MHz. The downlink phase noise requirements are 2.5 deg root mean square (rms) in the coherent mode and 2.8 deg rms in the noncoherent mode, when measured in a 10-Hz double-sided noise bandwidth DSN tracking receiver. The DST ranging and carrier phase delay variations over the flight acceptance (FA) temperature range (-10 to +55 deg C) are to be less than 22 nsec and 2.5 nsec, respectively. The differential downlink carrier phase delay variation is to be less than 1 nsec over the FA temperature range. The hardware qualification temperature range is from -20 to +75 deg C, with an expected flight operating range from +5 to +45 deg C. The hardware must withstand 15-krad (silicon) total radiation dose, 18.4-gravities (g) rms acceleration, 3000-g rms pyroshock, 12-g peak sine vibration, and 17.8-g rms random vibration environments.

III. Transponder

A. Block Diagram and Frequency Scheme

The DST frequency-generation scheme and functional block diagram are shown in Fig. 1. The receiver is implemented as a double-conversion, super-heterodyne, phase-lock tracking receiver, with a fixed-frequency second intermediate frequency (IF). The first local oscillator (LO) signal at 880 F_1 and the second LO signal at 131 $F_1 - F_2$ are generated by a dielectric resonator oscillator (DRO) [2,3] and a surface acoustic wave resonator oscillator (SRO), respectively. Both of these oscillators are phase locked to the 12 F_1 (114.75-MHz) voltage-controlled oscillator (VCO). The 12 F_1 VCO is in turn phase locked to the uplink carrier. The first and second intermediate frequencies are at 131 F_1 (1252.6875 MHz) and F_2 (56.648 MHz), respectively. Coherent carrier automatic gain control (AGC) is employed in both of the IF sections to provide a constant signal plus noise at the carrier loop phase detector.

The coherent downlink carrier at 880 F_1 is provided by the LO DRO when the DST is operating in the coherent mode from the VCO. In the noncoherent mode, an 880 F_1 frequency is generated by the exciter DRO phase locked to the DST 12 F_1 auxiliary oscillator or the external USO. The noncoherent downlink signal is automatically selected by the receiver AGC function in the absence of an uplink signal. The DST's 880 F_1 phase-modulated signal [4] provides drive for the redundant spacecraft power amplifiers.

B. Automatic Phase Tracking Loop

In the coherent mode, the 880 F_1 downlink signal generated in the DST exciter from the 12 F_1 VCO signal is phase coherent with the 749 F_1 received signal. Phase coherence is accomplished by an automatic phase-lock loop (PLL) in the receiver. The receiver PLL transfer function is a type-I, second-order lowpass filter [5,6]. The PLL design [5,6] is an involved iterative task and is usually a compromise between fast low-error tracking operation and noise response. The selection of the loop filter time constants (t_1 and t_2), the loop gain (K_V), and the noise equivalent pre-detection bandwidth (B_L), depends on six relevant receiver performance requirements. The requirements are:

(1) the steady-state tracking error equal to 1 deg per 40 kHz offset at carrier levels greater than -110 dBm

(2) the minimum acceptable signal-to-noise power ratio (SNR) in the carrier channel at the phase detector input equal to −25 dB

(3) the minimum acquisition sweep rate at a strong signal (> −110 dBm) equal to 550 Hz/sec

(4) the damping factor at the theoretical threshold of (−158 dBm) equal to 0.5

(5) the damping factor at 10 dB above the theoretical threshold equal to 0.8

(6) the two-sided loop noise bandwidth ($2B_{LO}$) at the theoretical threshold (−158 dBm) equal to 18 Hz

Using the above set of transponder performance requirements, the loop parameters t_1, t_2, and K_V are selected using a PLL algorithm. Physical limitations of the components are also considered in this selection. Table 2 lists these loop parameters and compares them for several transponders: NASA Standard, Galileo, and Magellan.

C. Residual Phase Noise

In the coherent carrier mode, residual phase noise is defined for a noise-free received signal case. Thus, phase noise on the downlink, unmodulated, carrier signal consists primarily of contributions from the three phase-locked oscillators 12 F_1 VCO, SRO, and DRO used in the DST implementation. Individual phase noise power spectral density functions [7,8,9] for these contributors are used in a comprehensive computer program to predict the phase noise of the closed-loop receiver. Total residual phase noise in the output is the mean square sum of all noise sources. The predicted phase noise for the DST in the coherent mode is shown in Fig. 2. In the intervals between 5 Hz and 25 MHz on each side of the carrier, the root mean square (rms) phase noise is 0.448 deg rms, which is well below the maximum allowable 2.5 deg for coherent downlink. The dominant contributor to this rms phase noise is the 12 F_1 VCO; the remaining contributions are less than 10 percent of the VCO contribution. Predicted rms phase noise and Allan deviation [8] are compared to the specified values in Table 3. The results of the analysis indicate that the coherent mode specifications will be met for both the rms phase noise and the Allan deviation. The closed-loop receiver servomechanism band limits the VCO spectrum, thus providing the superior performance in the coherent mode.

D. Carrier Delay and Delay Variation

The phase variation associated with the temperature change of the transponder can be estimated by constructing a model from the block diagram. The analysis assumes that the frequency multipliers are major contributors of the phase delay variation with temperature. The contribution for each multiplier is assumed to be three degrees of phase per degree Celsius. The estimated value of the DST carrier phase delay variations from input to output is equal to 0.075 nsec over the FA (−10 deg C to +55 deg C) temperature range. The predicted carrier delay data indicate that DST satisfies the requirement of maximum allowable delay variations equal to 2.5 nsec. Hardware performance characteristics over the temperature environment will be measured on an engineering model DST in 1991.

IV. Transponder Experimental Results

A breadboard DST X-band receiver and exciter shown in Fig. 1 (without S-band and Ka-band exciters) was implemented and performance characterization accomplished in both the Transponder Development Laboratory and the Telecommunications Development Laboratory (TDL). The evaluation measurements include receiver tracking threshold sensitivity, static phase errors for X-band (7162 MHz) uplink frequency offset, swept acquisition characteristics, and AGC versus uplink signal level. All measurements were made at room temperature (25 deg C). The measured tracking threshold sensitivity at the receiver best lock frequency (BLF) (approximately channel center) is −158 dBm, which is in good agreement with the design threshold value (−157.3 dBm) using the receiver loop noise bandwidth of 18 Hz and the measured LNA noise figure of 2.9 dB at 25 deg C. The measured receiver threshold characteristics show good correlation with expected performance over the tracking range as shown in Fig. 3. The receiver acquisition characteristics were measured at an input signal level of −110 dBm. The measured values for tracking range and tracking rate are ±270 kHz at design center frequency and 800 Hz/sec, respectively, and meet the specified requirements (Table 1). Figure 4 shows a linear relationship for the static phase error voltage versus uplink frequency offset over the receiver tracking range. The AGC loop-filter amplifier-output voltage controls the gain in the first and second intermediate frequency (IF) amplifiers. The AGC voltage versus uplink signal level at the best lock frequency and at frequency offsets (FOs) of ±250 kHz from BLF are shown in Fig. 5. As the receiver input signal varies from a strong signal level (−70 dBm) to the threshold level (−158 dBm), the AGC control voltage varies approximately linearly. No receiver false lock or self lock resulted during the test phase.

A comparison of measured to calculated phase jitter characteristics as a function of receiver uplink signal level is shown in Fig. 6. The TDL-system-measured residual phase jitter at a downlink signal level of −100 dBm with no uplink signal is equal to 2.62 deg rms. The TDL measured phase jitter values for the breadboard DST and Magellan transponders at the same uplink signal level of −100 dBm are equal to 3.03 deg rms and 3.98 deg rms, respectively (referred to the same 2.62 deg rms TDL system residual phase jitter).

V. Conclusions

Design concepts and system architecture for a high-performance X-band (7162-MHz/8415-MHz) DST for deep-space spacecraft applications have been presented. The DST has been successfully breadboarded and evaluated. New technologies such as a dielectric resonator oscillator, X-band (8415-MHz) phase modulator, and SRO have been integrated into the design. The Telecommunications Development Laboratory measurements on the breadboard DST achieved a threshold level of −158 dBm with a dynamic range of 88 dB and excellent acquisition and tracking characteristics. The measured tracking receiver threshold and phase jitter data are in good agreement with the predicted characteristics. The Jet Propulsion Laboratory breadboard X-band DST design and evaluation have demonstrated a basic model configuration for implementation of future deep-space transponders, and an engineering model development phase is expected to be completed by September 1991.

Acknowledgments

The authors gratefully acknowledge the valuable support by John T. Meysenburg for breadboard fabrication and testing, Peter W. Kinman for phase delay calculations, and Keith Siemsen of MOTOROLA (Strategic Electronics Division, Chandler, Arizona) for phase noise calculations.

References

[1] J. H. Yuen, *Deep Space Telecommunication Engineering*, New York: Plenum Press, 1983.

[2] N. R. Mysoor, "An Electronically Tuned, Stable 8415 MHz Dielectric Resonator FET Oscillator for Space Applications," *TDA Progress Report 42-93*, vol. January–March 1988, Jet Propulsion Laboratory, Pasadena, California, pp. 292–301, May 15, 1988.

[3] N. R. Mysoor, "An Electronically Tuned, Stable 8415 MHz Dielectric Resonator FET Oscillator for Space Applications," *Proc. IEEE 1990 Aerospace Applications Conference*, Vail, Colorado, pp. 147–156, February 5–9, 1990.

[4] N. R. Mysoor, "A Low-Loss Linear Analog Phase Modulator for 8415 MHz Transponder Applications," *TDA Progress Report 42-96*, vol. October–December 1988, Jet Propulsion Laboratory, Pasadena, California, pp. 172–178, February 15, 1989.

[5] F. M. Gardner, *Phaselock Techniques*, New York: John Wiley, 1979.

[6] A. Blanchard, *Phase-Locked-Loops: Applications to Coherent Receiver Design*, New York: John Wiley and Sons, 1976.

[7] D. B. Leeson, "A Simple Model of Feedback Oscillator Noise Spectrum," *Proc. IEEE,* vol. 54, pp. 329–330, February 1966.

[8] J. A. Barnes, A. R. Chi, and L. S. Cutler, *Characterization of Frequency Stability,* National Bureau of Standards Technical Note 394, Washington, D.C.: National Bureau of Standards, October 1970.

[9] D. W. Allan, "Time and Frequency (Time-Domain) Characterization, Estimation, and Prediction of Precision Clocks and Oscillators," *IEEE Transactions on Ultrasonics, Ferroelectronics, and Frequency Control,* vol. UFFC-34, no. 6, pp. 647–654, November 1987.

Table 1. Deep-space transponder specifications

Parameter	Design requirement
1. Uplink frequency allocation	7145 to 7190 MHz, deep space
2. Downlink frequency allocation	8400 to 8450 MHz, deep space
3. Frequency translation ratios	
Channel 14 uplink frequency	7162.3125 MHz (749 F_1)
X-band downlink	880/749 (8415 MHz)
S-band downlink	240/749 (2295 MHz)
Ka-band downlink	3344/749 (31,977 MHz)
4. Receiver parameters	
Carrier threshold	−157.3 dBm
Dynamic range	88 dB (carrier threshold to −70 dBm)
Noise figure at DST receiver input	2.5 dB maximum over −20 deg C to +75 deg C
Acquisition and tracking rate	550 Hz/sec at signal level > −110 dBm
Tracking range	±250 kHz minimum
Tracking error	< 1 deg/40 kHz at carrier level > −110 dBm
Capture range	±1.3 kHz at signal level > −120 dBm
5. Exciter parameters	
Frequency for coherent operation	880/749 time uplink frequency
Frequency for noncoherent operation	$\approx 880F_1$
RF output power level	+12 dBm, nominal
Output impedance	50 ± 5 ohms, nominal
Spurious signals	60 dBm below the carrier
Modulation bandwidth	> 40 MHz
Modulation index	Ranging: 3–9 dB carrier suppression Telemetry: 0–15 dB carrier suppression DOR: 0–1.1 dB carrier suppression
Modulation sensitivity	2 rad peak/volt peak
Modulation amplitude linearity	±2.5 rad at ±8 percent linearity
Modulation index stability	±10 percent over −20 deg C to +75 deg C
Residual phase noise	< 2.5 deg rms in the coherent mode < 2.8 deg rms in the noncoherent mode
Input-to-output carrier phase delay variation	< 2.5 nsec over −10 deg C to +55 deg C
Differential phase delay variation	< 1 nsec over −10 deg C to +55 deg C
Ranging phase delay variation	< 22 nsec over −10 deg C to +55 deg C

Table 2. Transponder carrier phase tracking loop parameters

Transponder	Design			Signal condition: Threshold, $\alpha_0 = 0.0531$			10 dB above threshold, $\alpha_{10} = 0.1665$			Strong signal, 50 dB above threshold, $\alpha_S = 1.0$			
	K_v, sec^{-1}	τ_1, sec	τ_2, sec	ζ_0	ω_{n_0}, rad/sec	$2B_{L_0}$, Hz	ζ_{10}	$\omega_{n_{10}}$, rad/sec	$2B_{L_{10}}$, Hz	ζ_S	ω_{n_S}, rad/sec	$2B_{L_S}$, Hz	$\Delta\omega$, Hz/sec
NST	1.44×10^7	2910	0.0833	0.68	16.23	17.0	1.20	40.3	28.7	2.90	70.3	209.9	394
NST + XSDC	4.77×10^7	2910	0.0833	1.90	45.28	92.0	3.34	273.9	80.2	5.40	128.0	697.1	1314
GLL	1.62×10^7	3732	0.0423	0.32	15.21	16.7	0.57	27.1	26.9	1.42	66.0	105.3	347
GLL + XSDC	5.73×10^7	3732	0.0423	0.73	34.09	36.6	1.30	90.0	60.4	2.66	123.9	341.2	1222
MAG	1.44×10^7	728	0.0208	0.42	40.38	41.0	1.49	118.3	71.5	1.50	126.0	210.0	1263
MAG + XSDC	4.9×10^7	728	0.0208	1.00	75.00	120.0	1.38	207.3	132.8	2.70	228.0	636.7	4136
DST	2.2×10^7	3556	0.0556	0.50	18.0	18.0	0.88	31.9	37.2	2.17	78.1	178.5	550

K_v = DC gain of the PLL, sec^{-1}
τ_1 = Time constant associated with the open-loop pole (phase lag) of the loop filter, sec
τ_2 = Time constant associated with the open-loop pole (phase lead) of the loop filter, sec
α_0, α_{10}, α_S = Limiter suppression factor at threshold, 10 dB above threshold, and strong signal
ζ_0, ζ_{10}, ζ_S = PLL damping factor at threshold, 10 dB above threshold, and strong signal
ω_{n_0}, $\omega_{n_{10}}$, ω_{n_S} = PLL natural frequency at threshold, 10 dB above threshold, and strong signal, rad/sec
$2B_{L_0}$, $2B_{L_{10}}$, $2B_{L_S}$ = PLL noise-equivalent bandwidth at threshold, 10 dB above threshold, and strong signal, Hz
$\Delta\omega$ = PLL acquisition and tracking rate at strong signal, Hz/sec
NST = NASA Standard DST (S-band)
GLL = Galileo transponder (S-band)
MAG = Magellan transponder (S-band)
DST = Deep space transponder (X-band design)
XSDC = External X-band to S-band downconverter

Table 3. Transponder coherent mode predicted rms phase noise and Allan deviation

	Predicted output	Specification
RMS phase noise (deg rms)	0.448	2.5 (5 Hz to 25 MHz)
Allan deviation (integration time):		
0.01 sec	2.6×10^{-11}	3×10^{-11}
1.0 sec	2.6×10^{-13}	1.2×10^{-12}
1000 sec	2.4×10^{-15}	5×10^{-15}

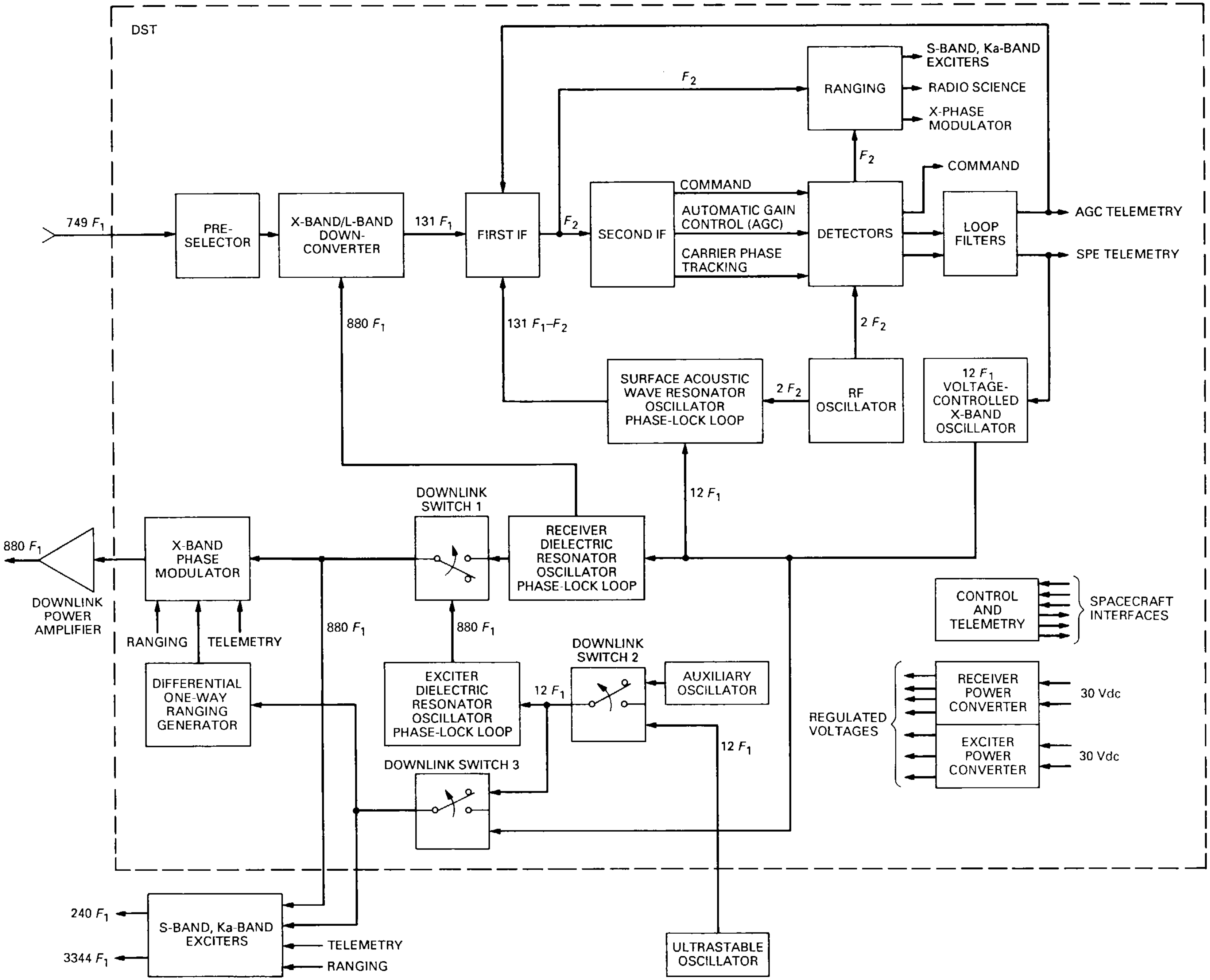

Fig. 1. Deep-space transponder.

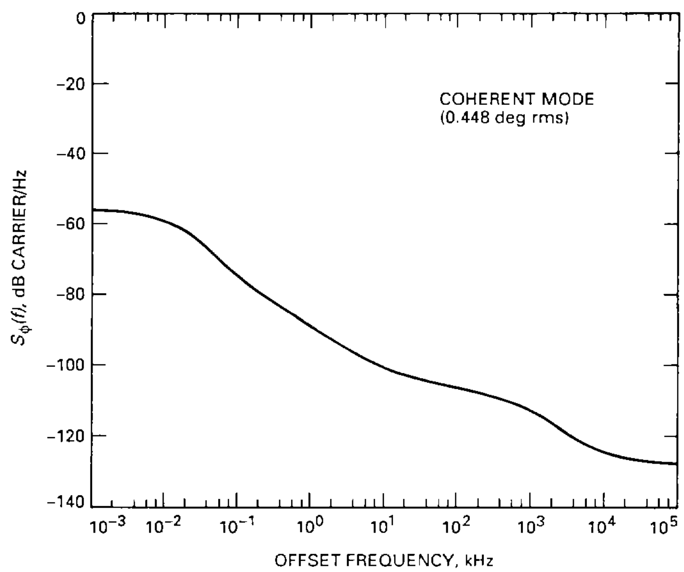

Fig. 2. DST 880 F_1 coherent mode phase noise.

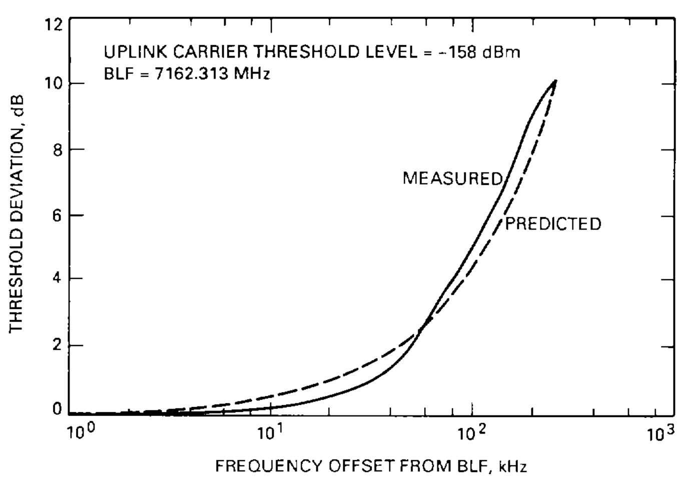

Fig. 3. DST carrier tracking threshold versus offset frequency.

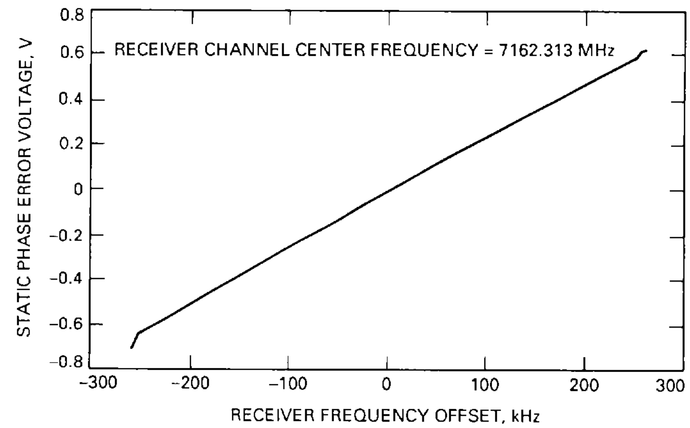

Fig. 4. DST static phase error voltage versus offset frequency.

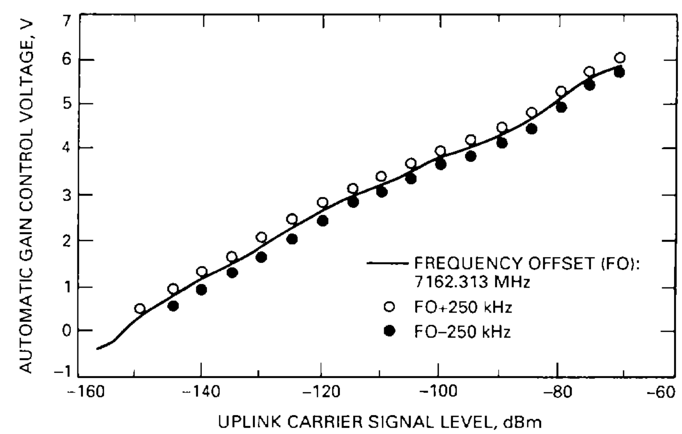

Fig. 5. DST AGC voltage versus uplink signal level.

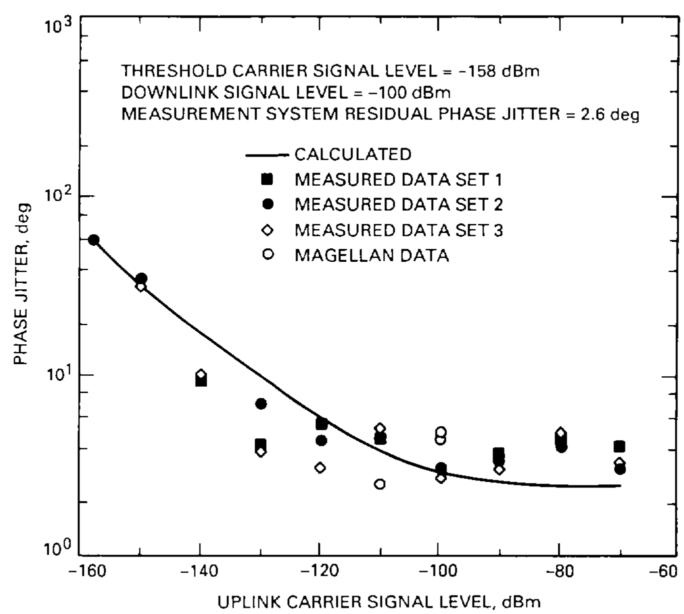

Fig. 6. DST phase jitter versus uplink signal level.